Appendix A. Supplementary data

Nickle Oxide Regulating Surface Oxygen to Promote Formaldehyde Oxidation on Manganese Oxide Catalyst

Hailin Zhao[a,†], Jie Tang[b,†], Zengyuan Li[a], Jie Yang[a], Hao Liu[a], Li Wang[a,], Yao Cui[b], Wangcheng Zhan[a], Yanglong Guo[a], Yun Guo[a,*]*

a Research Institute of Industrial Catalysis, School of Chemistry & Molecular Engineering, East China University of Science and Technology, Shanghai, 200237, P. R. China

b Technology Department, Shanghai HuaYi New Material Co., Ltd. 139 Pugong Road, Shanghai, 201507, P. R. China

[†] These two authors contributed equally to this paper.

[*] Corresponding Author: yunguo@ecust.edu.cn (Y. Guo), wangli@ecust.edu.cn (L. Wang)

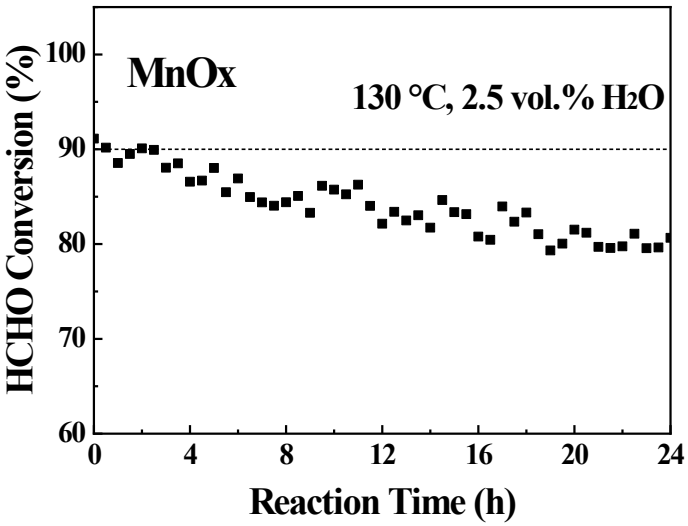

Fig. S1. Long-term stability of MnO_x at 130 ºC for 24 h, 300 ppm HCHO + 2.5 vol.% H_2O + Air.

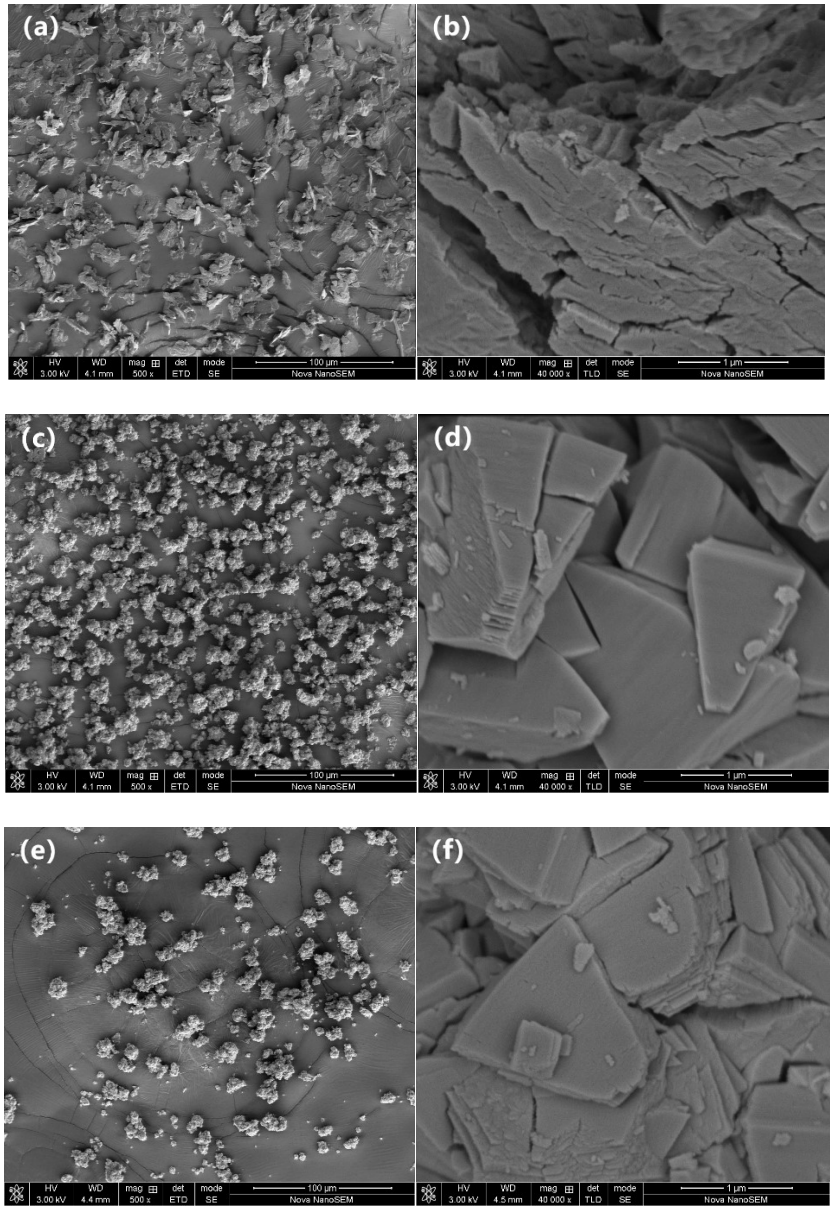

Fig. S2. FE-SEM images of MnO_x (a and b), 0.2NiO-MnO_x (c and d), and 0.4NiO-MnO_x (e and f) catalysts.

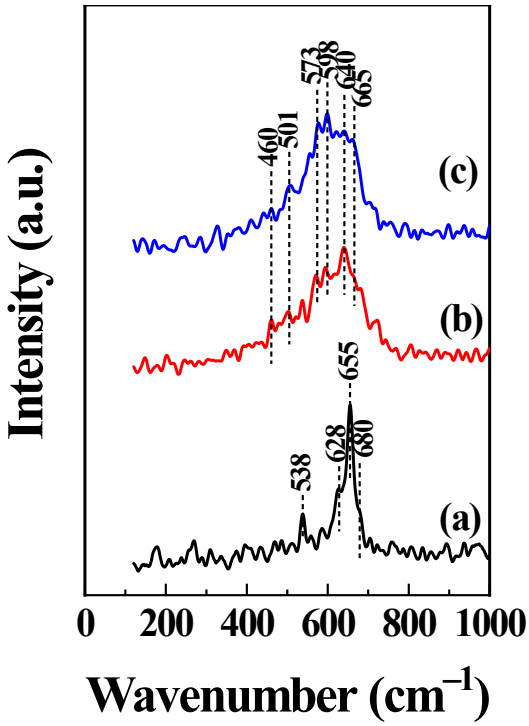

Fig. S3. Raman scattering spectra of (a) MnO_x, (b) 0.2NiO-MnO_x, and (c) 0.4NiO-MnO_x.

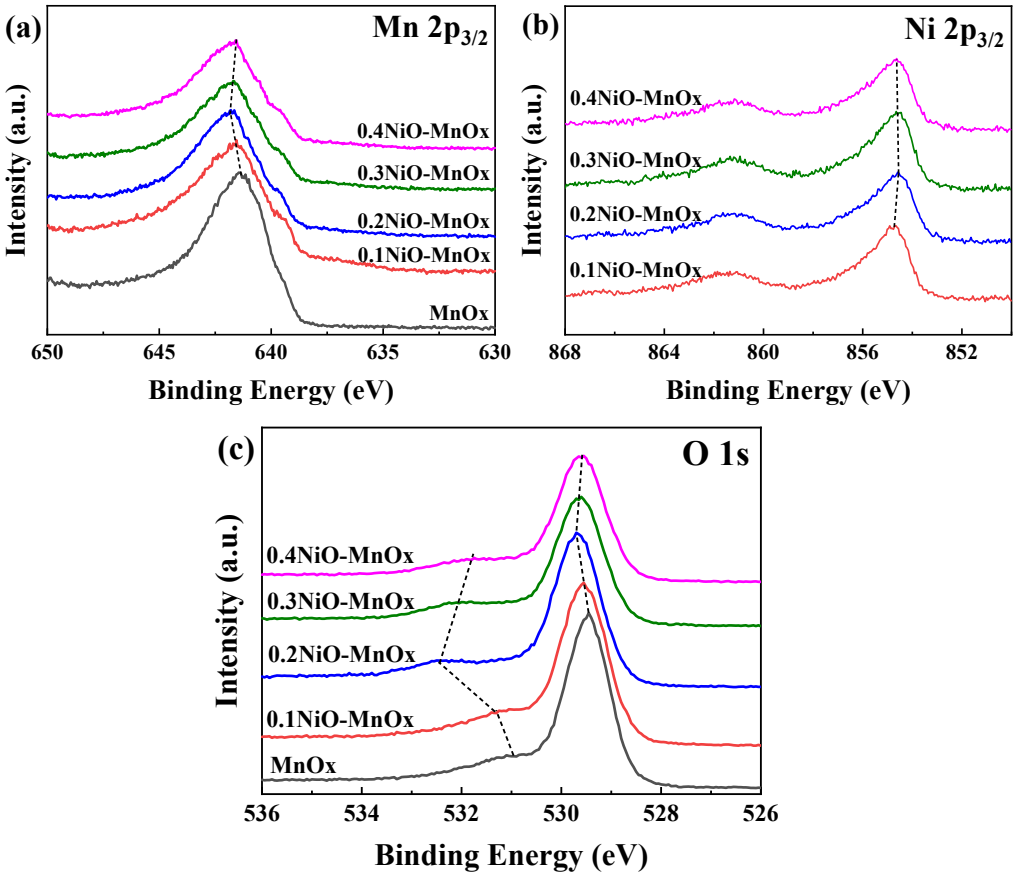

Fig. S4. XPS spectra of MnO_x and NiO-MnO_x samples: (a) Mn $2p_{3/2}$, (b) Ni $2p_{3/2}$ and (c) O 1s.

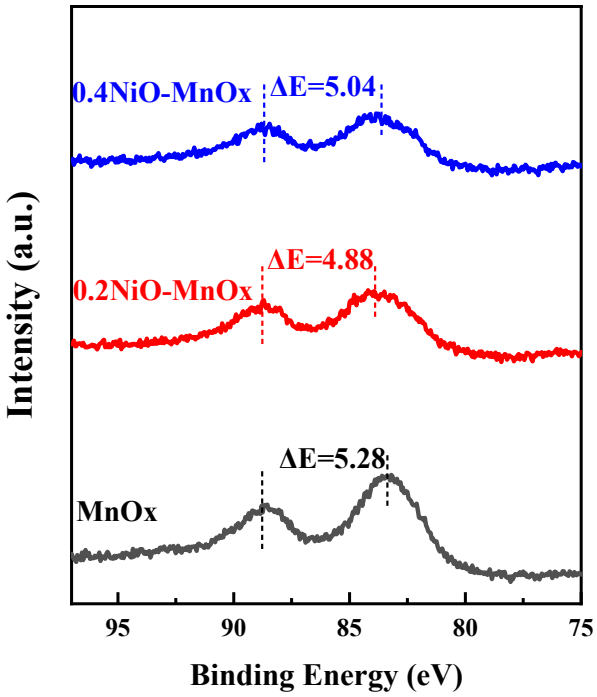

Fig. S5. Mn 3s spectra of MnO_x, 0.2NiO-MnO_x, and (c) 0.4NiO-MnO_x.

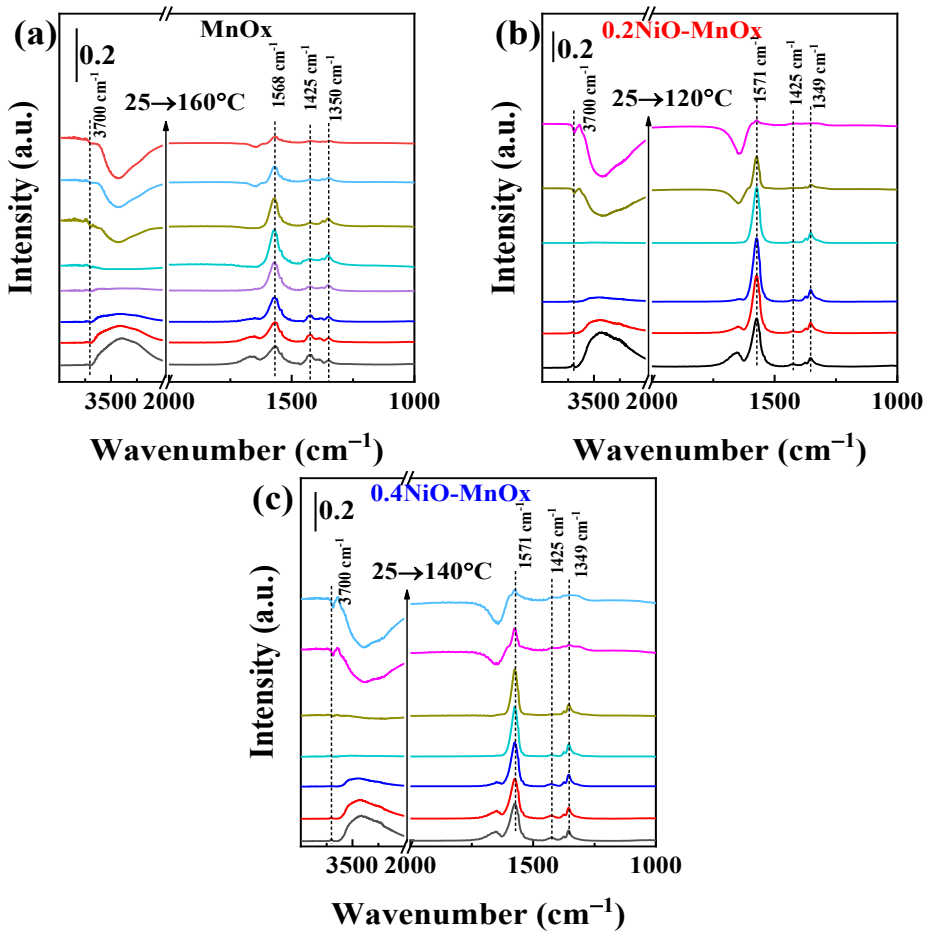

Fig. S6. In situ spectra of formaldehyde oxidation in 20% O_2/Ar with rising temperature over (a) MnO_x, (b) 0.2NiO-MnO_x, and (c) 0.4NiO-MnO_x after pre-adsorption.

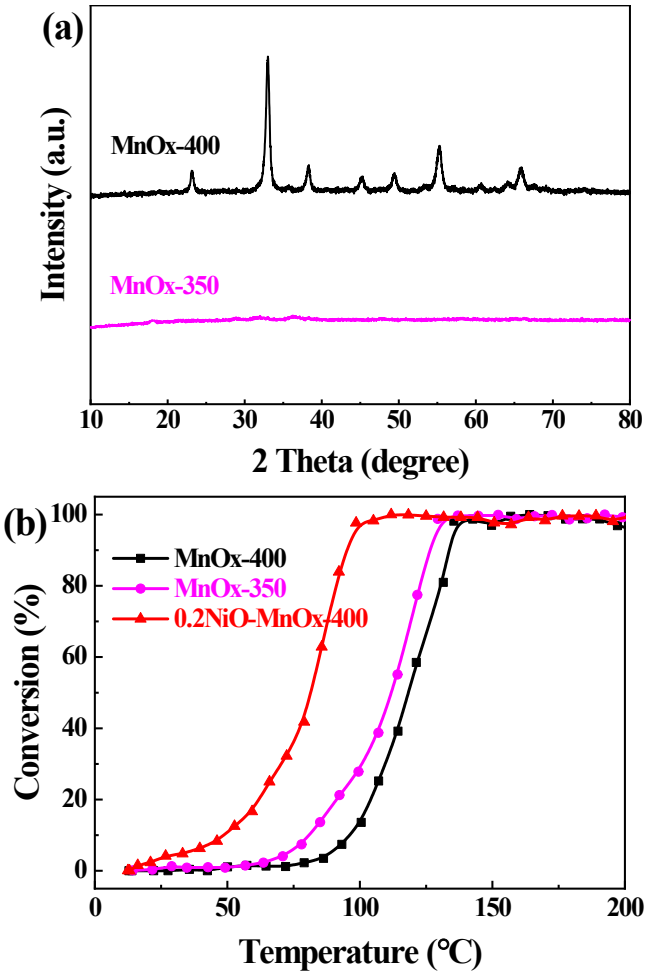

Fig. S7. (a) XRD patterns of MnO_x calcinated at 350 and 400 ºC; (b) formaldehyde oxidation activities of MnO_x-350, MnO_x-400, and 0.2NiO-MnO_x-400.

Since no diffraction peaks of MnO_x were observed in the XRD patterns of NiO-MnO_x, and amorphous MnO_x usually shows high activity, amorphous MnO_x was prepared and its activity was tested. MnO_x-350 catalyst was prepared by the similar method to MnO_x-400, the difference was the calcination temperature was 350 ºC. XRD patterns in Fig. S6(a) showed that MnO_x-350 was mainly in the amorphous phase. T_{50} and T_{90} of MnO_x-350 were 112 and 127 ºC, respectively, showing that formaldehyde oxidation activity of MnO_x-350 was a little higher than that of MnO_x-400 (T_{50} = 118 ºC, T_{90} = 134 ºC), but was far lower than that of 0.2NiO-MnO_x (T_{50} = 80 ºC, T_{90} = 94 ºC). Thus the difference in MnO_x crystallinity was not the key reason for the high activity of 0.2NiO-MnO_x.

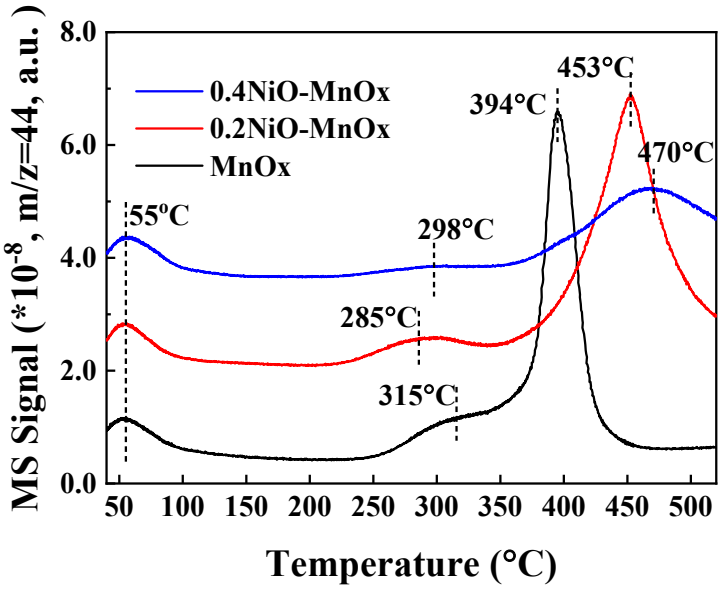

Fig. S8. CO_2-TPD profiles of as-prepared MnO_x, 0.2NiO-MnO_x, and 0.4NiO-MnO_x catalysts.

CO_2-TPD characterization for MnO_x, 0.2NiO-MnO_x, and 0.4NiO-MnO_x catalysts was carried out to research the surface basicity and CO_2 adsorption/desorption property, and the spectra are given in Fig. S7. CO_2 desorption peaks located at low temperature region (below 150 °C), medium temperature region (150–350 °C), and high temperature region (above 350 °C) are generally attributed to CO_2 adsorbed at weak, medium, and strong basic sites [1, 2]. All of the three samples showed a desorption peak with almost the same intensity at low temperature region, showing that CO_2 could desorb from the catalyst surface efficiently, that is quite important because if CO_2 did not desorb from the catalyst surface timely, it would occupy the active sites and deactivate the catalyst. The amount of CO_2 desorbed from medium and strong basic sites over 0.4NiO-MnO_x decreased dramatically compared to the other two samples, indicating that overmuch NiO doped into MnO_x can reduce basic sites and basic sites might be mainly provided by Mn species. The temperature order of medium intensity basic sites was 0.2NiO-MnO_x < 0.4NiO-MnO_x < MnO_x, which is the same as the activity order, may suggesting the relatedness between medium basic sites and activity, the weaker the medium basic sites are, the more favorable it is for formaldehyde oxidation product CO_2 to desorb from the catalyst surface.

Table S1. T_{50}, T_{90} and LTCC of MnO_x, NiO, and NiO-MnO_x catalysts with different Ni/(Ni + Mn) mole ratios for formaldehyde oxidation.

Sample	Catalytic activity (°C)		
	T_{50}	T_{90}	LTCC
MnO_x	118	134	139
0.1NiO-MnO_x	98	109	117
0.2NiO-MnO_x	80	94	98
0.3NiO-MnO_x	100	113	123
0.4NiO-MnO_x	107	125	133
NiO	152	180	188

Table S2. Formaldehyde oxidation activities over Mn-based catalysts in continuous flow test in recent years.

Catalysts	HCHO concentration	GHSV (mL/g·h)	T (°C)	Activity	Ref.
pyrolusite	400 ppm	30000	185	η=100%	[3]
cryptomelane			140		
todorokite			165		
K-OMS-2 (25 °C)	460 ppm	30000	100	η=64%	[4]
K-OMS-2 (100 °C)				η=10%	
birnessite MnO_2	100 ppm	50000	140	η=100%	[5]
cryptomelane			160	η=98%	
ramsdellite			160	η=97%	
MnOOH			160	η=96%	
birnessite MnO_2	200 ppm	120000	100	η=100%	[6]
MnO_2			120		
birnessite MnO_x (120 °C)	460 ppm	30000	100	η=100%	[7]
birnessite MnO_x (80 °C)			100	η=50%	
MnO_x-CeO_2 (MP)	580 ppm	21000	100	η=100%	[8]
MnOx-CeO_2 (SG)			180		
MnO_x–SnO_2 (RP)	400 ppm	30000	180	η=100%	[9]
MnO_x–SnO_2 (CP)			220		
birnessite MnO_2	40 ppm	120000	110	η=100%	[10]
20MnO_x/SBA-15	100 ppm	30000	160	η=90%	[11]
20MnO_x/SBA-15			175		
Graphene-MnO_2	100 ppm	30000	65	η=100%	[12]
MnO_2 hollow sphere	100 ppm	30000	113	η=100%	[13]
CoMn(3/1)-CP	80 ppm	60000	75	η=100%	[14]
CoMn(3/1)-CP			100		
$Co_{0.65}Mn_{2.35}O_4$	50 ppm	120000	100	η=100%	[15]
$Co_{0.78}Mn_{2.22}O_4$			140		
$Mn_{0.75}Fe_{3.30}$/AC	120 ppm	1500	240	η=90%	[16]
$Mn_{0.15}Fe_{3.30}$/AC				η=90%	
Na_1/HMO	140 ppm	120000	120	η=100%	[17]
HMO			140		
localized K^+ MnO_2	200 ppm	120000	110	η=100%	[18]
isolated K^+ MnO_2			145		
3D-MnO_2(dry air)	100 ppm	18000	120	η=100%	[19]
MnO_2 nanowire (dry air)			180		
MnO_x	300 ppm	40000	139	η=100%	This work
0.2NiO-MnO_x	300 ppm	40000	98	η=100%	

References

[1] X. Tang, F. Gao, Y. Xiang, H. Yi, S. Zhao, X. Liu, Y. Li, Effect of potassium-precursor promoters on catalytic oxidation activity of Mn-CoO_x catalysts for NO removal, Ind. Eng. Chem. Res., 54 (2015) 9116-9123.

[2] Z. Shang, M. Sun, X. Che, W. Wang, L. Wang, X. Cao, W. Zhan, Y. Guo, Y. Guo, G. Lu, The existing states of potassium species in K-doped Co_3O_4 catalysts and their influence on the activities for NO and soot oxidation, Catal. Sci. Technol., 7 (2017) 4710-4719.

[3] T. Chen, H. Dou, X. Li, X. Tang, J. Li, J. Hao, Tunnel structure effect of manganese oxides in complete oxidation of formaldehyde, Micropor. Mesopor. Mat., 122 (2009) 270-274.

[4] H. Tian, J. He, X. Zhang, L. Zhou, D. Wang, Facile synthesis of porous manganese oxide K-OMS-2 materials and their catalytic activity for formaldehyde oxidation, Micropor. Mesopor. Mat., 138 (2011) 118-122.

[5] L. Zhou, J. Zhang, J. He, Y. Hu, H. Tian, Control over the morphology and structure of manganese oxide by tuning reaction conditions and catalytic performance for formaldehyde oxidation, Mater. Res. Bull., 46 (2011) 1714-1722.

[6] J. Wang, G. Zhang, P. Zhang, Layered birnessite-type MnO_2 with surface pits for enhanced catalytic formaldehyde oxidation activity, J. Mater. Chem. A, 5 (2017) 5719-5725.

[7] H. Tian, J. He, L. Liu, D. Wang, Z. Hao, C. Ma, Highly active manganese oxide catalysts for low-temperature oxidation of formaldehyde, Micropor. Mesopor. Mat., 151 (2012) 397-402.

[8] X. Tang, Y. Li, X. Huang, Y. Xu, H. Zhu, J. Wang, W. Shen, MnO_x–CeO_2 mixed oxide catalysts for complete oxidation of formaldehyde: Effect of preparation method and calcination temperature, Appl. Catal. B: Environ., 62 (2006) 265-273.

[9] Y. Wen, X. Tang, J. Li, J. Hao, L. Wei, X. Tang, Impact of synthesis method on catalytic performance of MnO_x–SnO_2 for controlling formaldehyde emission, Catal. Commun., 10 (2009) 1157-1160.

[10] J. Wang, J. Li, C. Jiang, P. Zhou, P. Zhang, J. Yu, The effect of manganese vacancy in birnessite-type MnO_2 on room-temperature oxidation of formaldehyde in air, Appl. Catal. B: Environ., 204 (2017) 147-155.

[11] G. Rochard, C. Ciotonea, A. Ungureanu, J.-M. Giraudon, S. Royer, J.-F. Lamonier, MnOx loaded mesoporous silica for the catalytic oxidation of formaldehyde. Effect of the melt infiltration conditions on the activity–stability behavior, ChemCatChem, 12 (2020) 1664-1675.

[12] L. Lu, H. Tian, J. He, Q. Yang, Graphene–MnO_2 hybrid nanostructure as a new catalyst for formaldehyde oxidation, J. Phys. Chem. C, 120 (2016) 23660-23668.

[13] Y. Boyjoo, G. Rochard, J.-M. Giraudon, J. Liu, J.-F. Lamonier, Mesoporous MnO_2 hollow spheres for enhanced catalytic oxidation of formaldehyde, Sustain. Mater. Techno., 20 (2019) e00091.

[14] C. Shi, Y. Wang, A. Zhu, B. Chen, C. Au, $Mn_xCo_{3-x}O_4$ solid solution as high-efficient catalysts for low-temperature oxidation of formaldehyde, Catal. Commun., 28 (2012) 18-22.

[15] Y. Huang, K. Ye, H. Li, W. Fan, F. Zhao, Y. Zhang, H. Ji, A highly durable catalyst based on $Co_xMn_{3-x}O_4$ nanosheets for low-temperature formaldehyde oxidation, Nano Res., 9 (2016) 3881-3892.

[16] X. Du, C. Li, L. Zhao, J. Zhang, L. Gao, J. Sheng, Y. Yi, J. Chen, G. Zeng, Promotional removal of HCHO from simulated flue gas over Mn-Fe oxides modified activated coke, Appl. Catal. B: Environ., 232 (2018) 37-48.

[17] Y. Chen, J. Gao, Z. Huang, M. Zhou, J. Chen, C. Li, Z. Ma, J. Chen, X. Tang, Sodium rivals silver as single-atom active centers for catalyzing abatement of formaldehyde, Environ. Sci. Technol., 51 (2017) 7084-7090.

[18] J. Wang, J. Li, P. Zhang, G. Zhang, Understanding the "seesaw effect" of interlayered K^+ with different structure in manganese oxides for the enhanced formaldehyde oxidation, Appl. Catal. B: Environ., 224 (2018) 863-870.

[19] S. Rong, P. Zhang, Y. Yang, L. Zhu, J. Wang, F. Liu, MnO_2 framework for instantaneous mineralization of carcinogenic airborne formaldehyde at room

temperature, ACS Catal., 7 (2017) 1057-1067.